

NUMERICAL INVESTIGATION OF THE EFFECT OF THE INSULATION THICKNESS ON THE DEGREE OF NON-UNIFORMITY OF THE BILLET TEMPERATURE

by

Eakarach SOMRIEWWONGKUL and Chittin TANGTHIENG*

Department of Mechanical Engineering, Faculty of Engineering, Chulalongkorn University,
Pathumwan, Bangkok, Thailand

Original scientific paper
DOI: 10.2298/TSCI120419089S

The degree of non-uniformity of the billet temperature subjected to the radiative heat loss to the discharge door with different insulation thicknesses is investigated in this present study. The 2-D steady-state heat conduction for the billet subjected to different heat fluxes is solved by being transformed into a dimensionless form. The Gauss-Seidel iterative method for a finite volume discretization of the billet is employed to obtain the temperature distribution of the billet. The numerical result is validated by comparing with the field measurement data. A qualitative agreement between these two is observed. An effect of different insulation thicknesses on the heat-transfer characteristics and the degree of non-uniformity of the billet temperature is examined. In case of the replaced 50 mm thick insulation of the discharge door, the radiative heat loss to the discharge door is reduced by 49% with the replaced insulation, and the degree of non-uniformity of the billet temperature is decreased by 23 °C.

Key words: *reheating furnace, radiative heat loss, finite volume method, degree of non-uniformity, insulation thickness*

Introduction

In an iron and steel industry, a continuous reheating furnace is used for re-heating billets before being rolled to a finished product, such as steel bars, rods, or wires. It is basically divided into three zones: preheating, heating, and soaking zones. After a billet is preheated by hot exhaust gas, it is heated up by directed-fire burners to a desired temperature in the heating zone. Thereafter, the billet temperature uniformity between the surface and the core can be achieved in the soaking zone. The temperature uniformity is necessary to prevent any damage to the billet when being sent through the rolling process.

In order to estimate the billet temperature uniformity, numerous mathematical models have been proposed. A finite element model with an alternative direction implicit (ADI) method was used to predict the temperature profile of a slab in a pusher-type re-heating furnace with the maximum temperature deviation of 50 K at the middle cross-sectional plane [1]. In a study of Chen *et al.* [2], various heating rates of the furnaces were simulated by using a 2-D finite differ-

* Corresponding author; e-mail: qed690@yahoo.com

ence model. The result indicated that the temperature uniformity could be achieved faster in case of a higher heating rate. Hans *et al.* [3] indicated that the maximum temperature deviation inside a slab should be below 50 K before exiting the furnace. In their study, a finite volume method was employed to predict the heating characteristics of a slab with the maximum temperature deviation inside a slab of 400 K in the beginning of the heating zone whereas the degree of temperature uniformity was highly developed in the soaking zone. The maximum temperature deviation of the final slab was found to be 27 K. In a study of Kim [4], a 2-D transient heat conduction model of steel slabs in the five-zone walking beam furnace was developed. His result showed that the maximum temperature difference within a slab gradually decreases from approximately 340 K in the charging zone to 46 K in the soaking zone. It can be seen that these models have been developed for a furnace operated under a normal condition. However, because the discharged door of the furnace is regularly open, heat loss from thermal radiation through the discharged door may increase the degree of non-uniformity of the billet temperature.

Heat loss from thermal radiation through an opening has been extensively investigated by many researchers. It was estimated by Trinks *et al.* [5] by introducing the total radiative factor which is a function of the wall thickness and the opening shape. In the work of Ward and Probert [6], a heat diagram of the five-zone pusher-type furnaces was presented after the improvement of the insulation of the slab-support structure. The result showed that the radiation loss through the openings was up to 2.5%. Lyman [7] founded that the reduction of energy consumption by 41% of the reheating furnace could be achieved by the combination of several improvements, including the opening loss reduction and the insulation improvement. Both Vereshchagin *et al.* [8] and Si *et al.* [9] performed a heat balance on a furnace and indicated that heat loss through the furnace openings was approximately less than 1%.

Various numerical models based on the heat conduction equation to predict the billet/slab temperature distribution have been proposed. Since the heat transfer mechanism in the furnace is quite complicated, the 2-D heat conduction equation subjected to the radiative flux at the surfaces [10, 11] or the prescribed surface temperature with the spatial variation [2] is used to simplify the complexity. More complicated models such as a 3-D heat conduction equation coupled with the radiative transfer equation [4] or the 3-D heat conduction equation subjected to the gaseous radiation [1, 3] were presented. Since the heat loss through the openings does not have a significant effect on the heat transfer mechanism in the furnace, it is not necessary to use a complicated numerical model in this present study. Thus, the 2-D heat conduction equation subjected to the boundary conditions related to different heat losses is chosen to predict the effect of the heat loss through the open discharge door on the degree of non-uniformity of the billet temperature. The finite volume discretization is employed to obtain the numerical solution. A comparison between the billet temperature distributions obtained from the numerical prediction and that obtained from the field measurement is made. A replacement of the original door material with a thermal insulation with different thicknesses is considered to improve the degree of non-uniformity of the billet temperature. The variations of the non-uniformity with different values of the insulation thickness are investigated.

Problem formulation

In this study, the reheating furnace is an oil-fired pusher-type one as shown in fig.1. The study is focused on a billet located at the furnace exit on the x-y plane as shown in the end view of fig. 1.

The billet considered as a system under consideration is subjected to different heat fluxes as depicted in fig. 2. The dimensions of the billet are the length (L) of 2.42 m and the cross-sectional area ($W \times H$) of $0.1 \times 0.1 \text{ m}^2$.

To formulate the mathematical model, the major assumptions are made as follows: (1) the system is under a steady-state condition since the temperature profile of the billet at the furnace exit slightly changes with time [4,12]. (2) The problem can be assumed 2-D. (3) The problem can be considered axis symmetric on y -axis. (4) For the gas radiation, the grey-gas assumption is employed.

(5) For the surface radiation, the surfaces of the refractory wall and the billet are assumed grey. (6) The thermal properties of the billet are constants. From these assumptions, the 2-D steady-state heat conduction equation with associated boundary conditions can be written as:

$$\frac{\partial}{\partial x} \left(k \frac{\partial T}{\partial x} \right) + \frac{\partial}{\partial y} \left(k \frac{\partial T}{\partial y} \right) = 0 \quad (1)$$

$$x = 0; \quad \frac{\partial T}{\partial x} = 0 \quad (2)$$

$$x = \frac{L}{2}; \quad k \frac{\partial T}{\partial x} = q''_{\text{rad,g}} + q''_{\text{rad,w}} + q''_{\text{rad,d}} + q''_{\text{rad,\infty}} + q''_{\text{conv,a}} \quad (3)$$

$$y = 0; \quad T = T_f \quad (4)$$

$$y = H; \quad k \frac{\partial T}{\partial y} = q''_{\text{rad,g}} + q''_{\text{rad,w}} + q''_{\text{conv,g}} \quad (5)$$

Since the thermal conductivity of the billet (k) is a constant of 30 W/mK, eq. (1) is simplified to the 2-D Laplace equation. The boundary condition (4) represents the constant surface temperature on the furnace floor (T_f) of 1,060 °C. The right-hand side of eqs. (3) and (5) is the total heat transfer to the billet upper and end surfaces exposed to different heat fluxes, respectively. The detailed equations for these exposed heat fluxes are as follows.

The equation for gas radiation ($q''_{\text{rad,g}}$) has been developed by Hottel and Sarofim [13]:

$$q''_{\text{rad,g}} = \left[\frac{\varepsilon_b + 1}{1} (4 + a + b - c) \varepsilon_{\text{g,av}} \sigma T_{\text{av}}^3 \right] (T_g - T_s) \quad (6)$$

This equation is limited to a small temperature difference between the gas temperature (T_g) and the billet surface temperature (T_s). The value of T_g set to 1,250 °C. The exhaust gas emissivity (ε_g), which is a function of the emissivity of water and carbon dioxide, serving as major radiative components of the exhaust gas. The values of a , b , c , and $\varepsilon_{\text{g,av}}$ appearing in eq. (6) can be determined from [13]. The emissivity of the billet (ε_b) is set to 0.9.

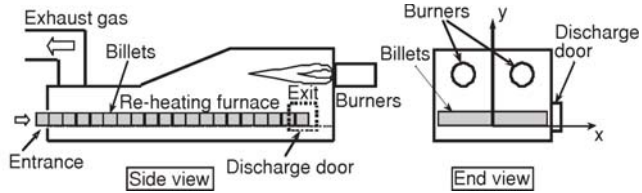


Figure 1. Schematic of a pusher-type re-heating furnace

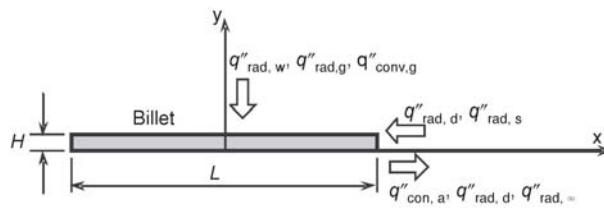


Figure 2. Billet under consideration subjected to different heat fluxes

The refractory wall radiation to the billet ($q''_{\text{rad,w}}$) can be determined by assuming the radiation exchange within the two-surface enclosure between the wall and the billet surfaces:

$$q''_{\text{rad,w}} = \frac{\sigma(T_w^4 - T_s^4)}{\frac{1}{\varepsilon_b} + \frac{A_b}{A_w} \left(\frac{1 - \varepsilon_w}{\varepsilon_w} \right)} \quad (7)$$

The view factor from the billet to the refractory wall is equal to unity. The surface emissivity of the refractory wall (ε_w) is set to 0.8. From the furnace geometry, the billet-to-wall area ratio (A_b/A_w) is 0.4525. The temperature of the refractory wall (T_w) in the re-heating furnace is generally less than T_g by approximately 100 °C [12]. Therefore, T_w is set to 1,150 °C.

The relation of the exhaust gas convection ($q''_{\text{conv,g}}$) can be determined by employing the basic Newton law of cooling. First, the mass flow rate of the exhaust gas is calculated by combining the fuel consumption rate and the combustion air mass flow rate. Then, the average exhaust gas velocity flowing above the upper surface of the billet is estimated. Finally, the correlation of the external flow over a flat plate is utilized to determine the average convective heat transfer coefficient of the exhaust gas (h_g). As a result, h_g can be estimated to be 25.7 W/m²K.

Since the discharge door is not well insulated, this results in the radiative heat loss from the end surface of the billet to the discharge door ($q''_{\text{rad,d}}$). When the discharge door is closed, the radiative heat loss to the discharge door can be written as:

$$q''_{\text{rad,d}} = (1 - C)F_{\text{bd}}\varepsilon_b\sigma(T_d^4 - T_s^4) \quad (8)$$

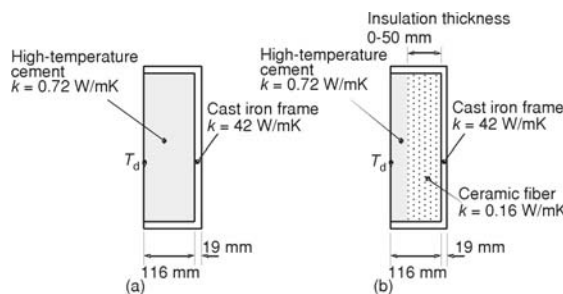


Figure 3. Discharge door: (a) with original materials, (b) with ceramic fiber insulation

(8), the value of the average inner surface temperature of the discharge door (T_d) as shown in fig. 3 must be determined. Because the outer surface temperature of the discharge door and the surrounding temperature can be obtained from the field measurement, T_d can be estimated by calculating the heat flux through the discharge door using the 1-D steady-state heat conduction equation. As a result, T_d in case of the discharge door with original materials is 998 K whereas that in case of the discharge door with replaced ceramic fiber insulation varies from 998 to 1,204 K as the insulation thickness increases from 0 to 50 mm.

When the discharge door is open, the radiative heat loss to the surrounding ($q''_{\text{rad},\infty}$) through the openings can be written as:

$$q''_{\text{rad},\infty} = CF_{\text{b}\infty}\varepsilon_b\sigma(T_\infty^4 - T_s^4) \quad (9)$$

F_b is the average view factor of the billet to the surroundings, which is identical to F_{bd} . The average surrounding temperature (T_∞) is measured to be 34.4 °C.

The C represents the open time fraction of the discharge door. F_{bd} is the average view factor of the billet to the door, which is considered as a view factor of parallel rectangular plates [14]. The values of C and F_{bd} are 0.275 and 0.691, respectively. A schematic diagram of the discharge door made of the original materials and replaced ceramic fiber insulation is depicted in fig. 3. The detailed explanation of the discharge door improvement will be described in the next section. In order to utilizing eq.

Leak air convection ($q''_{\text{conv,a}}$) is caused by the leak air flowing into the furnace due to the negative furnace pressure. The amount of the leak air can be measured by comparing the percentage of oxygen in the exhaust gas when the discharge door is open with that when the discharge door is closed. Once the mass flow rate of the leak air has been determined, the leak air convection can be estimated by calculating the leak air convective heat transfer coefficient (h_a) using the basic Newton law of cooling. Consequently, the calculated value of h_a is $4.7 \text{ W/m}^2\text{K}$.

Numerical solution procedure

To facilitate the numerical solution procedure, the co-ordinate transformation is performed by introducing the dimensionless variables as follows:

$$\xi = \frac{x}{H}, \quad \eta = \frac{y}{H}, \quad \theta = \frac{T - T_f}{T_g - T_f} \quad (10)$$

Substituting the eq. (10) into eqs. (1) to (5) yields:

$$\frac{\partial^2 \theta}{\partial \xi^2} + \frac{\partial^2 \theta}{\partial \eta^2} = 0 \quad (11)$$

$$\xi = 0; \quad \frac{\partial \theta}{\partial \xi} = 0 \quad (12)$$

$$\xi = 12.1; \quad \frac{\partial \theta}{\partial \xi} = \text{Bi}_{\text{rad,g}}(1 - \theta) + \text{Bi}_{\text{rad,w}}(\theta_w - \theta) + \text{Bi}_{\text{rad,d}}(\theta_d - \theta) + (\text{Bi}_{\text{rad,\infty}} + \text{Bi}_{\text{conv,a}})(\theta_\infty - \theta) \quad (13)$$

$$\eta = 0; \quad \theta = 0 \quad (14)$$

$$\eta = 1; \quad \frac{\partial \theta}{\partial \eta} (\text{Bi}_{\text{rad,g}} + \text{Bi}_{\text{conv,g}})(1 - \theta) + \text{Bi}_{\text{rad,w}}(\theta_w - \theta) \quad (15)$$

The radiative and convective Biot numbers (Bi_{rad} and Bi_{conv}) are defined as:

$$\text{Bi}_{\text{rad}} = \frac{h_{\text{rad}}H}{k}, \quad \text{Bi}_{\text{conv}} = \frac{h_{\text{conv}}H}{k} \quad (16)$$

The dimensionless governing eq. (11) with associated boundary conditions (12) to (15) is solved numerically by the finite volume method. A schematic diagram of a uniform grid arrangement is shown in fig. 4. A common discretization technique by performing the local heat balance on each finite volume cell is employed [15]. The proper grid size of $\Delta\xi$ and $\Delta\eta$ will be discussed later. After a system of linear equations is constructed, the Gauss-Seidel method is used to solve these linear equations [16]. The linearized coefficients, which include the radiative heat transfer coefficient term, are updated by a simple iterative algorithm. When the convergence criteria of the billet temperature profile and the linearized coefficients of 10^{-10} are met, the numerical solution is obtained.

To improve the degree of uniformity of the billet temperature, some part of the discharge-door original material made of high-temperature cement must be replaced

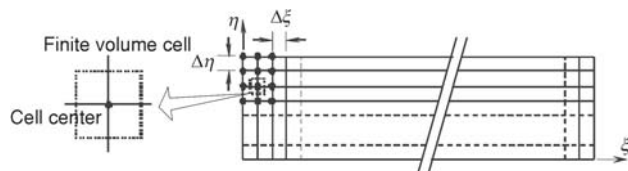


Figure 4. Grid arrangement for the finite volume discretization

by ceramic fiber insulation with much lower value of the thermal conductivity as given in fig. 3. In this study, the insulation thickness is viewed as a parameter varies from 0 to 50 mm. To protect the ceramic fiber insulation from the direct flame radiation from the burners, the high-temperature cement is still used to cover the insulation surface with the overall thickness remaining at 116 mm. It should be noted that in practice, only one thickness value will be chosen by the manufacturer. The improvement of the degree of the billet temperature uniformity will reduce the chance of roll breakage leading to the reduction of the waste product. The compensation between the cost of the waste reduction and the investment cost of the insulation is not included in the scope of this study and should be further investigated.

Grid independence of the numerical results is examined for difference values of $\Delta\xi$ and $\Delta\eta$. The values of $\Delta\xi$ and $\Delta\eta$ is set to be equal for simplicity. By comparing to the smallest grid sizes of $\Delta\xi = \Delta\eta = 0.025$, it is found that for $\Delta\xi = \Delta\eta = 0.05, 0.1, 0.2$, the relative errors of the temperature distribution in the billet are less than 0.08, 0.18, and 1.38% with the computational time of 960, 120, and 7 second, respectively. Thus, the grid size of $\Delta\xi = \Delta\eta = 0.1$ is chosen to perform the numerical computation with sufficient accuracy.

Results and discussion

To verify the numerical prediction, the actual billet temperatures are obtained from the field measurement by a thermal imaging camera located at the furnace exit. The thermal images with a resolution of 384×288 pixels are captured immediately after the billet is discharged from the furnace. The surface temperature of the billet measured by the camera has an uncertainty of $\pm 2\%$. Comparison between the temperature distributions predicted by the numerical model and that obtained by the field measurement is depicted in fig. 5.

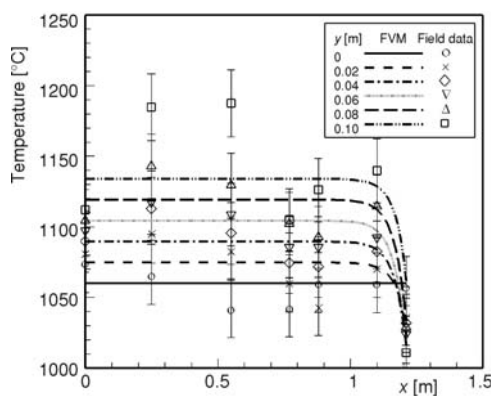


Figure 5. Comparison between the temperature distributions obtained from the numerical prediction and the field

temperature. The similar behavior of the temperature drop at the vicinity near the billet tip is also observed from the field measurement. Therefore, the minimum temperature of the entire billet is located at its end surface, which is exposed to the radiative heat loss to the discharge door and to the environment.

To understand the heat-transfer characteristics of the entire billet, the heat balance diagrams of the billet in case of the discharge door with original materials and with 50-mm-thick ceramic fiber insulation are illustrated and compared in fig. 6. In case of the discharge door with

It can be seen that the numerical result and the field data are in qualitative agreement. However, the result obtained by the field measurement indicates the temperature fluctuation, especially at the upper surface of the billet, *i. e.*, at $y = 0.1$ m. The hot spot is caused by a location of the burners that provide non-uniform heat fluxes to the billet upper surface. It is noticed that the magnitude of the fluctuation is lower as y is decreased further away from the upper surface. The maximum relative error of the temperature obtained from these two methods is 4.7%. At a given value of y , the numerical results indicates the uniform temperature starting from $x = 0$ until the appearance of the temperature drop beyond $x = 1$, resulting in a higher degree of non-uniformity of the billet

original materials shown in fig. 6(a), the amount of combined gas and refractory wall radiation is approximately 88% whereas the amount of gas convection is the remaining 12%. The agreement of this result can be found in references [4, 17] where the radiation dominates the heat-transfer mechanism within the furnace. The majority of heat loss, the floor conduction, is approximately 74% of the total heat input. The radiative heat loss to the discharge door and the surrounding is approximately 15 and 9%, respectively. From eqs. (7) and (8), although T_{∞} is much less than T_d , the open time fraction (C) of 27.5% leads to the lower value of $q''_{rad,\infty}$ compared to that of $q''_{rad,d}$. It is noted that the effect of the leak air convection on the total heat output is negligible. On the other hands, by comparing the heat balance diagrams shown in fig. 6(a) and fig. 6(b), all parts of the input heat, *i. e.*, the gas radiation, the wall radiation, and the exhaust gas convection, do not have much change. In contrast, the significant effect of the replaced insulation on the radiative heat loss to the discharge door is observed: it is reduced by 49%. However, since the contribution of the radiation to the discharge door to the total heat is less than 20%, the total amount of heat transferred into and out of the billet marginally is decreased by 2.9%.

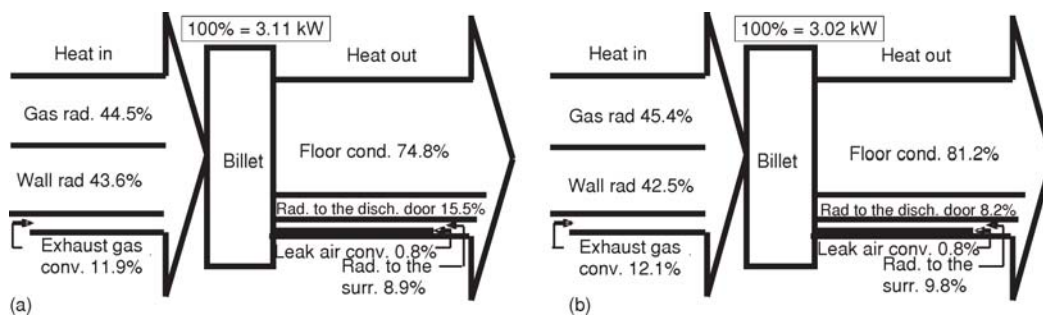


Figure 6. Heat balance diagram of the billet in case of the discharge door with (a) original materials, (b) 50-mm-thick ceramic fiber insulation

To investigate the degree of non-uniformity of the billet temperature, the temperature deviation is defined as the magnitude of the temperature difference between the maximum and minimum values of the entire billet [3, 18]. It can be seen from fig. 5 that the maximum billet temperature is located on the upper surface of $y = 0.10$ m. Since the change of the insulation thickness does not have significant effect on the input heat, the maximum billet temperature in any case of all insulation thicknesses remains almost the same at 1,134 °C. On the other hand, the minimum billet temperature is located at the billet end surface of $x = 1.21$ m. To determine the exact location of the minimum billet temperature, the temperature profiles at the billet end surface for different insulation thicknesses are illustrated in fig. 7.

It can be seen that the minimum billet temperature is located in the middle along the y -axis. For given insulation thicknesses of 0, 25, and 50 mm, the minimum temperature is ap-

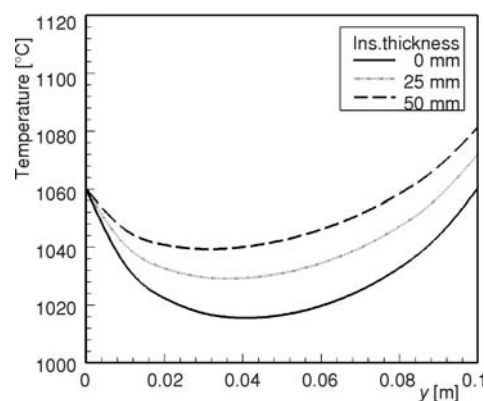


Figure 7. Temperature profile at the billet end surface for different insulation thicknesses

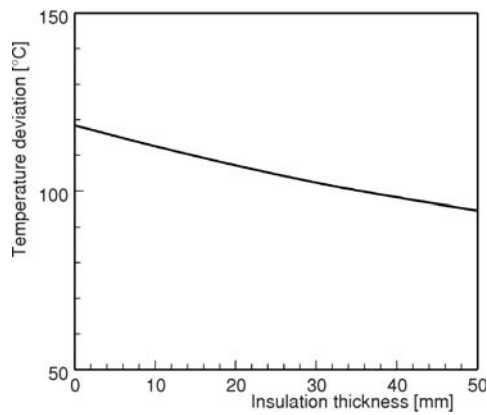


Figure 8. Variation of the temperature deviation with different insulation thicknesses

top and bottom firing, in which the heat can be distributed more evenly [1, 3, 4]. However, since the furnace under consideration is equipped with two top firing burners only, it is rather difficult to fulfill this requirement.

Conclusions

A numerical prediction to investigate the effect of the insulation thickness on the degree of non-uniformity of the billet temperature has been proposed in this study. The 2-D steady-state heat conduction equation for the billet subjected to different heat fluxes at the billet surfaces is presented and transformed into a dimensionless form. It is numerically solved by employing the finite volume method with the Gauss-Seidel iterative technique. To reduce the degree of non-uniformity of the billet temperature, the replacement of the original materials with ceramic fiber insulation is proposed. To verify the validity of the numerical results, a comparison between the numerical prediction and field data results in a qualitative agreement. The heat-transfer characteristics of the billet are investigated by performing the heat balance over the entire billet. When 50-mm-thick ceramic fiber insulation is used instead of the original materials of the discharge door, the radiative heat loss to the discharge door is reduced by 49% whereas the total amount of heat transferred into and out of the billet is decreased by 2.9%. The temperature deviation, representing the degree of non-uniformity of the billet temperature, is decreased from 118 to 95 °C. The benefit of the reduction of the temperature deviation is to reduce the chance of roll breakage due to end splitting.

Nomenclature

A – area, [m²]
 Bi – Biot number ($= hH/k$), [-]
 F – view factor, [-]
 H – billet height, [m]
 h – convective heat transfer coefficient, [Wm⁻²K⁻¹]
 k – thermal conductivity of the billet, [Wm⁻¹K⁻¹]
 L – billet length, [m]
 q – heat flux, [Wm⁻²]

T – temperature, [°C] or [K]
 W – billet width, [m]
 x, y – Cartesian co-ordinate, [m]

Greek symbols

ε – emissivity, [-]
 ξ, η – dimensionless co-ordinate in x- and y- axes, [-]
 θ – dimensionless temperature, [-]
 σ – Stefan-Boltzmann constant, [Wm⁻²K⁻⁴]

proximately 1,016, 1,029, and 1,039 °C located at $x = 0.4, 0.35,$ and 0.3 m, respectively. Once the maximum and minimum billet temperatures are obtained, the temperature deviation with different insulation thicknesses can be calculated and depicted in fig. 8. It is noticed that the temperature deviation is decreased from 118 to 95 °C with increasing insulation thickness from 0 to 50 mm. The reduction of the temperature deviation caused by the temperature drop at the billet end is one of the factors that reduces the chance of roll breakage due to end splitting. In practice, it is recommended as a guideline for the manufacturer to keep the temperature deviation below 50 °C [3, 19]. This requirement can be achieved in case of a reheating furnace with

Subscripts

a	– leak air	g	– gas
av	– average	rad	– radiation
b	– billet	s	– surface
conv	– convection	w	– refractory wall
d	– discharge door	∞	– surrounding
f	– floor		

References

- [1] Lindholm, D., Leden, B., A Finite Element Method for Solution of the Three-Dimensional Time-Dependent Heat Conduction Equation with Application for Heating of Steels in Reheating Furnaces, *Numerical Heat Transfer, Part A: Applications*, 35 (1999), 2, pp. 155-172
- [2] Chen, W. H., *et al.*, Analysis on Energy Consumption and Performance of Reheating Furnaces in a Hot Strip Mill, *International Communication in Heat and Mass Transfer*, 32 (2005), 5, pp. 695-706
- [3] Han, S. H., *et al.*, Transient Radiative Heating Characteristics of Slabs in a Walking Beam Type Reheating Furnace, *International Journal of Heat and Mass Transfer*, 52 (2009), 3-4, pp. 1005-1011
- [4] Kim, M. Y., A Heat Transfer Model for the Analysis of Transient Heating of the Slab in a Directed-Fired Walking Beam Type Reheating Furnace, *International Journal of Heat and Mass Transfer*, 50 (2007), 19-20, pp. 3740-3748
- [5] Trinks, W., *et al.*, *Industrial Furnaces*, 6th ed., John Wiley and Sons Inc., New York, USA, 2004, pp 189-192
- [6] Wart, J., Probert, S. D., Reduction of Energy Losses Associated with Stock Support Structures in Slab-Reheating Furnaces, *Applied Energy*, 1 (1975), 3, pp. 223-236
- [7] Lyman, B., Energy Saving in Reheating Steel Billets in Improved Furnace Facility, *Industrial Heating*, 49 (1982), 4, pp. 20-21
- [8] Vereshchagin, A. V., *et al.*, Reducing Heat Loss in Pusher-Type Continuous Reheating Furnace, *Metallurgist*, 51 (2007), 9-10, pp. 505-506
- [9] Si, M., *et al.*, Energy Efficiency Assessment by Process Heating Assessment and Survey Tool (PHAST) and Feasibility Analysis of Waste Heat Recovery in the Reheat Furnace at a Steel Company, *Renewable and Sustainable Energy Reviews*, 15 (2011), 6, pp. 2904-2908
- [10] Jang, Y. J., Kim, S. W., An Estimation of a Billet Temperature during Reheating Furnace Operation, *International Journal of Control, Automation, and Systems*, 5 (2007), 1, pp. 43-50
- [11] Guo-Jun, L., *et al.*, The Simplified Method to Calculate Two-Dimensional Heat Conduction Equations of Heating Slab, *Applied Mechanics and Materials*, 79 (2011), July, pp. 105-110
- [12] Jaklic, A., *et al.*, Online Simulation Model of the Slab-Reheating Process in a Pusher-Type Furnace, *Applied Thermal Engineering*, 27 (2007), 5-6, pp. 1105-1114
- [13] Hottel, H. C., Sarofim, A. F., *Radiative Transfer*, McGraw-Hill Inc., New York, USA, 1967, pp. 299-301
- [14] Ehlert, J. R., Smith, T. F., View Factors for Perpendicular and Parallel Rectangular Plates, *Journal of Thermophysics and Heat Transfer*, 7 (1993), 1, pp. 173-175
- [15] Incropera, F. P., DeWitt, D. P., *Fundamentals of Heat and Mass Transfer*, 5th ed., John Wiley and Sons, New York, USA, 2002, pp. 198-201
- [16] Patankar, S. V., *Numerical Heat Transfer and Fluid Flow*, Taylor and Francis, USA, 1980, pp. 47-48
- [17] Huang, M. J., *et al.*, A Coupled Numerical Study of Slab Temperature and Gas Temperature in the Walking-Beam-Type Slab Reheating Furnace, *Numerical Heat Transfer, Part A*, 54 (2008), 6, pp. 625-646
- [18] Chen, W. L., *et al.*, Experimental and Theoretical Investigation of Surface Temperature Non-Uniformity of Spray Cooling, *Energy*, 36 (2011), 1, pp. 249-254
- [19] Dutta, S., Hot Rolling Practice – An Attempted Recollection, <http://www.steel-insdag.org>

Paper submitted: April 19, 2012

Paper revised: June 11, 2014

Paper accepted: July 18, 2014